PAPER

Dynamics and heat diffusion of Abrikosov's vortex-antivortex pairs during an annihilation process

IOP Publishing Journal of Physics: Condensed Matter
J. Phys.: Condens. Matter **29** (2017) 405605 (9pp) https://doi.org/10.1088/1361-648X/aa81e6

Dynamics and heat diffusion of Abrikosov's vortex-antivortex pairs during an annihilation process

E C S Duarte[1], E Sardella[2], W A Ortiz[3] and R Zadorosny[1]

[1] Departamento de Física e Química, Universidade Estadual Paulista (UNESP), Faculdade de Engenharia de Ilha Solteira, Caixa Postal 31, 15385-000 Ilha Solteira-SP, Brazil
[2] Departamento de Física, Universidade Estadual Paulista (UNESP), Faculdade de Ciências, Caixa Postal 473, 17033-360, Bauru-SP, Brazil
[3] Departamento de Física, Universidade Federal de São Carlos—UFSCar, 13565-905, São Carlos-SP, Brazil

E-mail: rafazad@gmail.com

Received 2 March 2017, revised 18 July 2017
Accepted for publication 25 July 2017
Published 4 September 2017

Abstract

The manipulation and control of vortex states in superconducting systems are of great interest in view of possible applications, for which mesoscopic materials are good candidates. In this work, we studied the annihilation dynamics and the dissipative aspects of an Abrikosov's vortex-antivortex pair in a mesoscopic superconducting system with a concentric hole. The generalized time-dependent Ginzburg–Landau equations were numerically solved. The main result is the appearance of a phase slip-like line due to the elongation of the vortex and antivortex cores. Under specific circumstances, thermal dissipation might be associated with a sizeable relaxation of the order parameter, so that the energy released in the annihilation of a vortex-antivortex pair might become detectable in measurements of the magnetization as a function of time.

Keywords: vortex dynamics, TDGL, annihilation, heat diffusion, energy dissipation

(Some figures may appear in colour only in the online journal)

1. Introduction

The study of vortex matter is an issue of greatest interest, since the comprehension and manipulation of the vortex motion are very important for possible applications as in the case of control of spins by vortices [1–3]. However, unusual behaviors appear when the vortices are subjected to an environment where the confinement effects emerge, as is the case of mesoscopic systems. As an example, we cite the formation of multivortex states, where one has coexistence of single and giant vortices[4]. In mesoscopic systems, this state tends to follow the geometry of the sample [4–12]. Also, due to interactions between vortices and the shielding currents, the formation of a giant vortex is conceivable under certain circumstances. In this case, the cores of individual vortices collapse into a single entity with vorticity greater than one [13–17].

On the other hand, under specific conditions, it is possible that a vortex-antivortex pair (V–AV) becomes stable. Such stability has a close correspondence with the symmetry of the system, e.g. it is possible to stabilize a state with vorticity 3 in a square system by 4 vortices located near the vertices and an antivortex in the center of the square [18]. The V–AV dynamics was also studied in systems with holes [19–21], magnetic dots [22–25] and arrays of small current loops [26].

The V and AV can be spontaneously formed after a quench caused by, e.g. a hot spot [27, 28]. In this scenario, as the heat is diffused and depending on the velocity of such diffusion, the vortices are arranged in a cluster or in a metastable ring-like configuration [27]. In a ring superconductor, just after a quench, there is no interaction of the Vs and the

[4] A giant vortex is a multiquanta vortex with a single core.

AVs with the defects and annihilations occur. After such a period of time, some Vs and AVs leave the sample or are trapped in the ring's hole, which generates a magnetic flux inside the hole [28].

In [29, 30], the nucleation and penetration of vortices were studied in very thin films and wires under applied currents and magnetic fields. In such cases, the vortices penetrate the samples forming a chain in the thin films and helicoidal lines in the wires [29]. It was also shown that the normal state penetrates the superconductor like macroscopic droplets which in the presence of defects evolve to single vortices [30].

Samples with a V–AV state were also studied by Berdiyorov and coworkers [31]. They analyzed the V–AV dynamics in a thin stripe with electric contacts where a current was injected. In this system a phase slip line is formed and the annihilation of V and AV depends on the intensity of the applied current. This annihilation process produces an oscillating voltage over the contacts in a terahertz frequency [31]. In this sense, it is interesting to mention the work of Gulevich and Kusmartsev [32] who proposed a device based on a long annular Josephson junction where the creation, annihilation and trapping of flux and antiflux take place. The authors claim that their device is very sensitive and could become a detector of microwave radiation and magnetic fields.

In [20], Sardella and coworkers, analyzed the annihilation of a V–AV pair in a square mesoscopic system with a concentric square hole. As a result, it was shown that, when the vortex is entering the system, its average velocity is of the order of 10^3 m s^{-1} and, during the annihilation motion, due to the mutual attraction between the V and the AV, its average velocity reaches values of the order of 10^5 m s^{-1}. Recently, Zadorosny *et al* [21] studied similar systems and have shown that the V–AV pair acquires an elongated shape which creates a channel between the border of the system and the hole. In the analysis of the V–AV pair motion it was also shown that such specimens acquire an acceleration in the early and final stages of the annihilation process, with a nearly constant velocity motion between these stages.

In practice, mesoscopic superconducting materials have been applied in devices like amplifiers [33], imaging of single magnetic flux quantum (single vortex) [34], single electron [35] and single photon [36–39] detectors, and the knowledge of the V–AV dynamics in such materials is of great importance to improve specific characteristics to those applications.

In this work we studied the annihilation process between a vortex and an antivortex in mesoscopic superconducting square systems with a concentric square hole. The study is focused on a systematic analysis of the parameters for which the annihilation process occurs in the superconducting region. Attention is also given to the total energy released in such a collision. Our results indicate that the energy generated in such process can be associated to frequencies in the infrared spectrum and also that smaller systems present the higher energies. We speculate that such system could be the heart of a future device for detection of electromagnetic waves in the appropriate frequency range.

This work is organized as follows. In section 2 we briefly delineate the theoretical formalism used to simulate the mesoscopic systems. In section 3 we present the results obtained from the simulations and, subsequently, discuss them. In section 4, we present our conclusions.

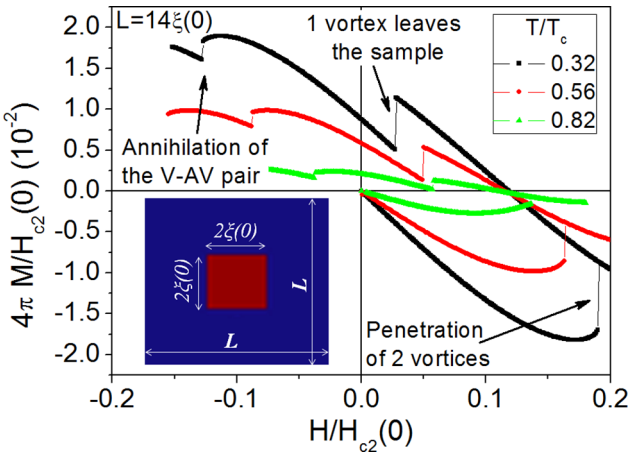

Figure 1. Magnetization as a function of the applied magnetic field for the $L = 14\xi(0)$ system. In such sample, two vortices are nucleated in the first penetration. In the decreasing field branch, one vortex is untrapped and leaves the sample and in the branch of negative fields the annihilation of the V–AV pair takes place. The inset shows an illustration of the simulated system.

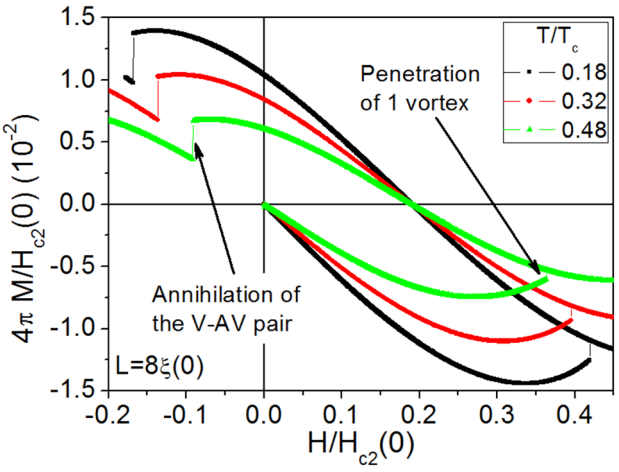

Figure 2. Magnetization as a function of the applied magnetic field for the $L = 8\xi(0)$ system. In such sample, only one vortex is nucleated in the first penetration and the annihilation of the V–AV pair takes place in the branch of negative fields.

2. Theoretical formalism

The time-dependent approach for the Ginzburg–Landau equations, proposed by Schmid [40], provides a temporal evolution of the order parameter ψ and the vector potential $\mathbf{A}$ for a superconducting material submitted to an external applied magnetic field and/or a transport current. Such approach is appropriate to describe most phenomena which occur in the resistive state. For our purposes, it will be important to use the equations for the energy dissipated due to both the induced electrical field and the relaxation of ψ during the vortex motion. It is worth to mention that this theoretical framework has a satisfactory agreement with experiments at temperatures

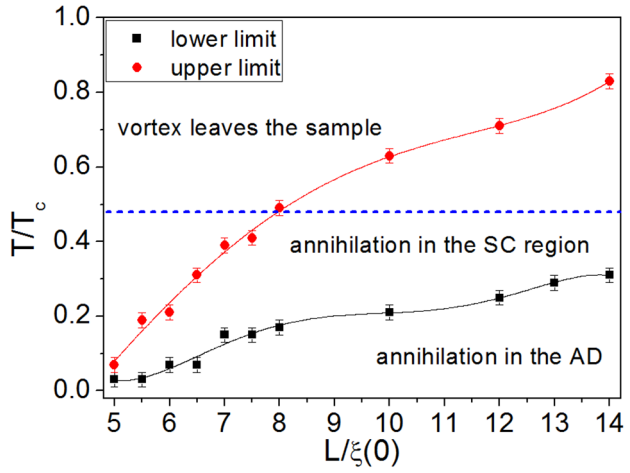

Figure 3. The $T(L)$ diagram indicating the domains for which the annihilation of a V–AV pair occurs in the superconducting region. The lines which links the points are only a guide for the eyes. The dashed line indicates the temperature, i.e. $T = 0.48T_c$, for which we analyzed the dynamics of the simulated systems.

larger than $T = 0.5T_c$ [40, 41] however, qualitatively explains the dynamics at lower temperatures. Those equations have also been applied in studies with induced voltage [42], magnetoresistance [43, 44] and the application of alternating external magnetic fields [45]. The equations proposed by Schmid were extended for gap superconductors by Kramer and Watts-Tobin [46]. Thus, the generalized time-dependent Ginzburg–Landau (GTDGL) equations take the form:

$$\frac{u}{\sqrt{1+\gamma^2|\psi|^2}}\left(\frac{\partial}{\partial t}+\frac{\gamma^2}{2}\frac{\partial|\psi|^2}{\partial t}+\mathrm{i}\varphi\right)\psi = -(-\mathrm{i}\boldsymbol{\nabla}-\mathbf{A})^2\psi+\psi(1-T-|\psi|^2), \tag{1}$$

$$\left(\frac{\partial\mathbf{A}}{\partial t}+\boldsymbol{\nabla}\varphi\right) = \mathbf{J}_s-\kappa^2\boldsymbol{\nabla}\times\boldsymbol{\nabla}\times\mathbf{A}, \tag{2}$$

where the superconducting current density is given by:

$$\mathbf{J}_s = \mathrm{Re}\left[\bar{\psi}(-\mathrm{i}\boldsymbol{\nabla}-\mathbf{A})\psi\right]. \tag{3}$$

Here, the distances are in units of the coherence length at zero temperature $\xi(0)$, the magnetic field is in units of the bulk upper critical field $H_{c2}(0)$, the temperature is in units of T_c, time is in units of $t_{GL}(0) = \pi\hbar/8k_bT_cu$, the Ginzburg–Landau time, $\mathbf{A}$ is in units of $H_{c2}(0)\xi(0)$, φ is the scalar potential and is in units of $\hbar/2et_{GL}(0)$, $\kappa = \lambda(0)/\xi(0)$ is the Ginzburg–Landau parameter, where $\lambda(0)$ is the London penetration length at zero temperature, and the order parameter is in units of α_0T_c/β, where α_0 and β are the phenomenological Ginzburg–Landau parameters [20]. The parameter u is related to the relaxation of ψ [47] and is very important in studies with dissipative mechanisms; u is extracted from a microscopic derivation of the Ginzburg–Landau equations using the Gor'kov approach [48, 49]. Frequently, $u = 5.79$ is adopted, as determined by first principle in [46]. In such formulation the inelastic phonon-electron scattering time, t_e, is taken into account and $\gamma = 2t_e\psi_0/\hbar$. The GTDGL equations were

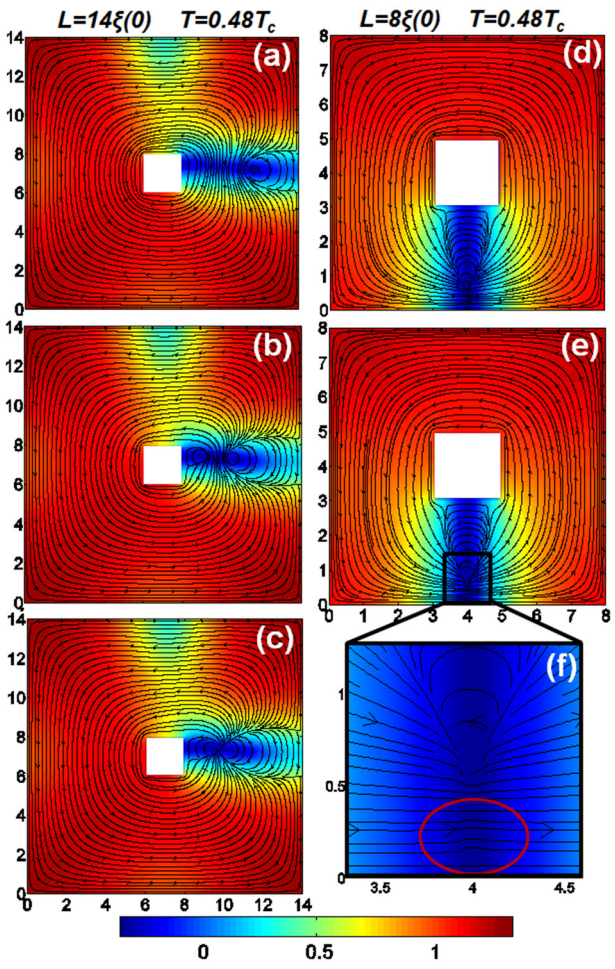

Figure 4. Intensity of $|\psi|$ during the annihilation process at $T = 0.48T_c$. The black lines indicate the superconducting currents flowing around the system. From panel (a) to (c), it shows the dynamics for $L = 14\xi(0)$: in (a) an AV penetrates the system with a V trapped in the hole; (b) the vortex leaves the hole and in (c) it is shown the overlap of the currents during the annihilation. From panel (d) to (f), it is shown the dynamics for $L = 8\xi(0)$. It is worth to note that in this case the dynamics occurred near the upper threshold line shown in figure 3. In (d) the V moves toward the border of the system; in (e) an AV starts to penetrate the system and (f) is a zoom showing the distortion of the currents due to the nucleation of an AV. It is also shown that the currents circumvents the vortex and/or the antivortex in such a way it forms a cone-like profile.

numerically solved by using the link-variable method [50, 51] which ensures the gauge invariance under the transformations $\psi' = \psi e^{i\chi}$, $\mathbf{A}' = \mathbf{A}+\boldsymbol{\nabla}\chi$, $\varphi' = \varphi-\partial\chi/\partial t$, when they are discretized in a numerical grid [52]. Therefore, for all times and positions we have chosen $\varphi' = 0$, since neither charges nor external currents are considered in this work. The equation for the dissipated power energy was obtained by using the Helmholtz free energy theorem for a superconductor in an external magnetic field [40, 45]. Such equation, in dimensionless form, is given by:

$$W_{total} = 2\left(\frac{\partial\mathbf{A}}{\partial t}\right)^2+\frac{2u}{\sqrt{1+\gamma^2|\psi|^2}}\left[\left(\left|\frac{\partial\psi}{\partial t}\right|\right)^2+\frac{\gamma^2}{4}\left(\frac{\partial|\psi|^2}{\partial t}\right)^2\right]. \tag{4}$$

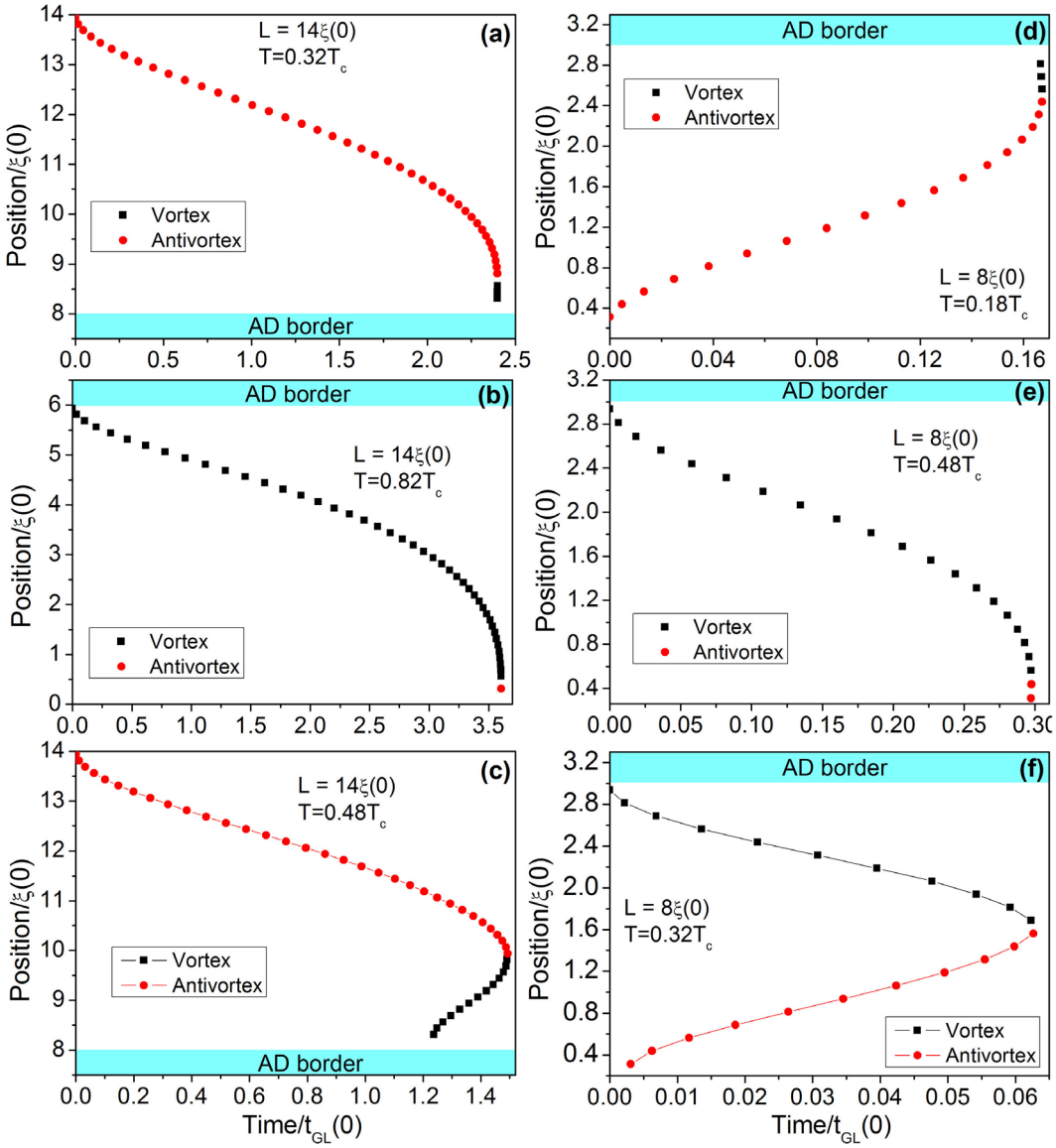

Figure 5. Position as a function of time in temperatures near the lower and upper threshold line of figure 3. (a) $T = 0.32T_c$, (b) $T = 0.82T_c$ for $L = 14\xi(0)$ system and (d) $T = 0.18T_c$, (e) $T = 0.48T_c$, for $L = 8\xi(0)$. (c) $0.48T_c$ and (f) $0.32T_c$ show the motion of the pair for an intermediate temperature for the systems $L = 14\xi(0)$ and $L = 8\xi(0)$, respectively.

The first term is the dissipation due to the induced electrical field, $W_{\mathbf{A}}$, and the second one is due to the dissipation related to the relaxation of the order parameter, W_ψ. The dissipated power energy is given in units of $H_{c2}^2(0)/[8\pi\kappa^2 t_{\mathrm{GL}}(0)]$. As W_{total} diffuses through the system, we couple the thermal diffusion equation to the GTDGL ones. By using the approach of [42], the dimensionless form of the thermal equation can be written as:

$$C'_{\mathrm{eff}}\frac{\partial T}{\partial t} = K_{\mathrm{eff}}\,\nabla^2 T + \frac{1}{2}W_{\mathrm{total}} - \eta(T - T_0). \qquad (5)$$

Here, η is the heat transfer coefficient of the substrate, $C'_{\mathrm{eff}} = \pi^4/48u$ is the effective heat capacity, and $K_{\mathrm{eff}} = \pi^4/48u^2$ is the effective thermal conductivity.

In the first part of this work, as we do not take into account dissipative effects, we set $u = 1$ and $\gamma = 0$ in equation 1. Such procedure is still well accepted in the literature [43] due to the good qualitative description of experimental data [53–55] and facilitated computations [20]. In the second part of the study, where the thermal dissipation and diffusion need to be properly taken into account, $u = 5.79$ and $\gamma = 10$ were used.

3. Results and discussion

We divide the discussion into two distinct scenarios. First, we consider the temperature constant throughout the system. And second, we take into account the heat diffusion produced by the V–AV collision.

3.1. Constant temperature

The simulations of the annihilation dynamics were carried out by adopting $u = 1$ and $\kappa = 5$. The value for κ is equivalent to those of some low critical temperature superconductors, such as the metallic alloy Pb–In [56]. The systems were simulated

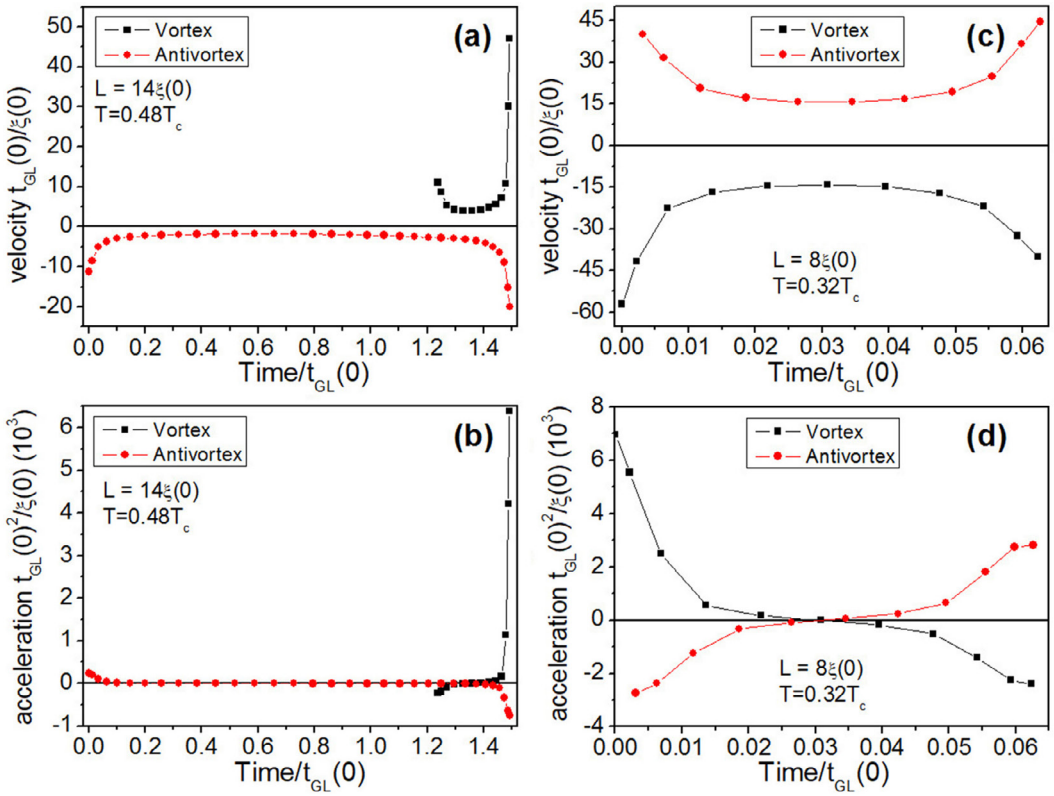

Figure 6. Velocities and accelerations of the vortex and antivortex motion for the $L = 14\xi(0)$ and $L = 8\xi(0)$ systems.

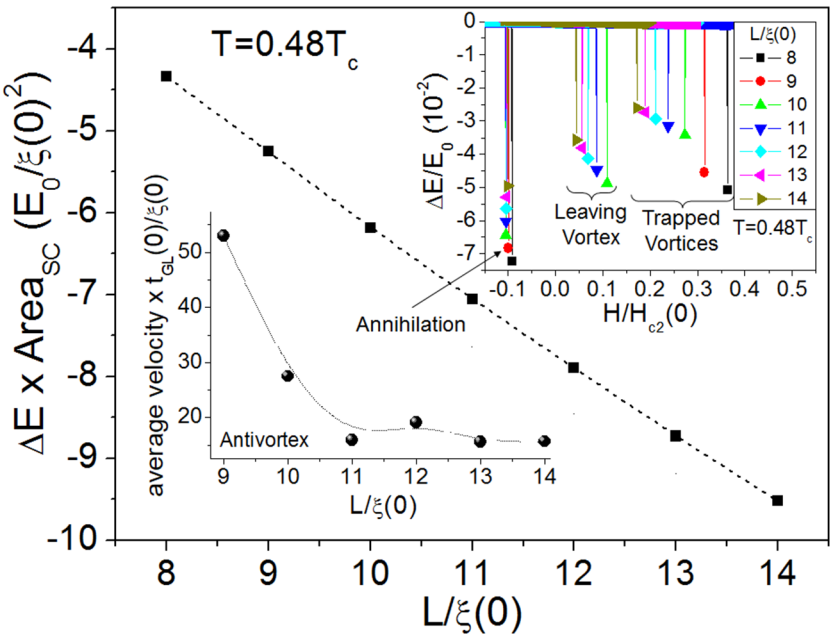

Figure 7. The main curve shows the variation of the normalized superconducting energy $\times$ the normalized superconducting area as a function of the lateral size of the system. The ΔE was calculated as the difference between the superconducting energy immediately before and just after the annihilation. The energy minimized in the annihilation process decreases as the size of the sample is increased. The upper inset shows ΔE as a function of the applied magnetic field for several systems at $T = 0.48T_c$. In the range $0.15 < H/H_{c2} < 0.4$ the vortices are trapped in the hole; for $0 < H/H_{c2} < 0.14$ one of the vortices is untrapped and leaves the sample. The dips around $H = -0.1H_{c2}$ occurs as the minimization of the energy after the annihilation. The lower inset shows the average velocity as a function of the lateral size of the systems. A quasi-phase slip line is formed in smaller systems as a consequence of the size effect. In such degraded region, the V–AV pair moves faster than in larger systems where the degradation does not take all the superconducting track.

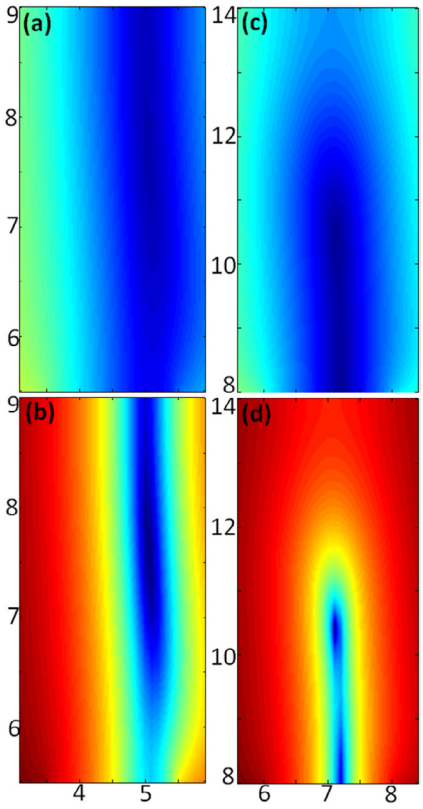

Figure 8. Upper panels: intensity of the order parameter, $|\psi|$; lower panels: for a better visualizing of the degraded superconducting region, we show $\log|\psi|$. In (a) and (b) we show the snapshots for the $L = 9\xi(0)$ system. From these panels, it can be clearly seen that no preserved superconducting region remains, once the values of $v_{\rm avg}$ are very large. On the other hand, for the $L = 14\xi(0)$ system is visible in both images (panels (c) and (d)) that there is still a superconducting region which is not entirely degraded. All snapshots were taken at the instant just before the annihilation of the V–AV pair.

with a concentric square hole of side $l = 2\xi(0)$, as shown in the inset of figure 1. For each system, the external magnetic field was varied in steps of $\Delta H = 10^{-3}H_{c2}(0)$ and the temperature in steps of $\Delta T = 0.2T_c$.

Figure 1 shows the magnetization versus applied magnetic field, $M(H)$ curves for the system with $L = 14\xi(0)$ at different temperatures. In this case, two vortices nucleate into the sample being trapped by the hole. As H is decreased, one vortex leaves the system and, when the field is inverted, an AV penetrates the sample while a vortex remains trapped in the hole. Thus, a V–AV pair is formed and each specimen moves toward each other until their mutual annihilation. The same process occurs in smaller systems as can be seen in figure 2 for a system with $L = 8\xi(0)$. The main difference is that in the first penetration only one vortex is nucleated and trapped by the hole. It is interesting to note that the annihilation process was detected even in systems with an effective superconducting region smaller than the size of a vortex core, i.e. smaller than $2\xi(0)$. Our simulations show that, in this case, both V and AV elongate to accommodate themselves into the superconducting material, so that the cores run against each other in a straight track, resembling a phase slip line, even though the order parameter is not exactly zero along this line. This aspect will be further discussed ahead in this paper.

In order to determine the parameters, such as the range of temperatures and the lateral sizes of the system, for which the annihilation process takes place in the superconducting region, a $T(L)$ diagram was built and the result is shown in figure 3. As described in this figure, below the line characterized by square symbols, namely, the lower limit, when H is inverted, the V remains trapped in the hole. Then, an AV penetrates the system and moves toward the center of the sample. The penetrated AV and the trapped flux interact attractively, what causes an acceleration of the AV, which falls in the hole and cancels the flux which was already inside. On the other hand, above the upper limit (circles), when H is inverted, the V is untrapped and leaves the sample before the nucleation of an AV. In between such lines, the annihilation of the V–AV pair occurs in the superconducting region.

The horizontal line in figure 3 indicates the isothermal where annihilation dynamics were analyzed. In figure 4 we exhibit some images of the intensity of $|\psi|$ which summarize the annihilation process for systems with two distinct sizes, i.e. $L = 14\xi(0)$—figures 4(a)–(c)—and $L = 8\xi(0)$—(d) to (f)—at $T = 0.48T_c$.

One can notice that in both systems a quasi phase slip line is formed[5]. Such region appears due to the attraction between the vortex and the antivortex which causes an elongation of their cores [21]. After the annihilation, such line disappears. In small systems, the hole and the border of the sample are so close that the distortion of the vortex and the antivortex, which occurs during their encounter, is sufficient to create such a quasi phase slip line. Figure 4 shows the intensity plot of $|\psi|$ and the black lines indicate the shielding currents. We can also notice that for both systems a visible structure is formed by the currents, which is originated in the drag motion of the V–AV pair. In figure 4(f), one of the borders of that system is zoomed up. We can see the distortion of the shielding current caused by the nucleation of an AV. To study the dynamics of the V–AV motion, in figure 5 we plotted the time evolution of the position of those specimens. The evolution of the $L = 14\xi(0)$ system is depicted in panels figures 5(a)–(c) for three distinct temperatures: in panel (a) it is basically shown the motion of the AV which annihilates the vortex near the hole in the vicinity of the lower limit $T = 0.32T_c$ of the phase diagram of figure 3; in panel (b) we show the vortex motion near the upper limit line $T = 0.82T_c$ where the annihilation occurs near the border; and finally in panel (c) the motion of an intermediate temperature is shown. The same evolution is illustrated in panels 5(d)–(f) for the $L = 8\xi(0)$ system at $T = 0.18T_c$, $0.48T_c$, and $0.32T_c$, respectively.

By calculating the derivatives of the curves from figure 5 (panels (c) and (f)) we obtained the velocity and the acceleration of the V–AV pair (see figure 6). It becomes evident that the motion of the pair is accelerated. The amplitude of the average velocity of the AV, as an example, decays and reaches a nearly constant value as the size of the system is increased,

[5] A phase slip line is a line along which the order parameter vanishes. This is clearly not the case in the present scenario. However, we can see that the order parameter is very small in a quite elongated region. It is in this sense that we use the denomination *quasi phase slip line*.

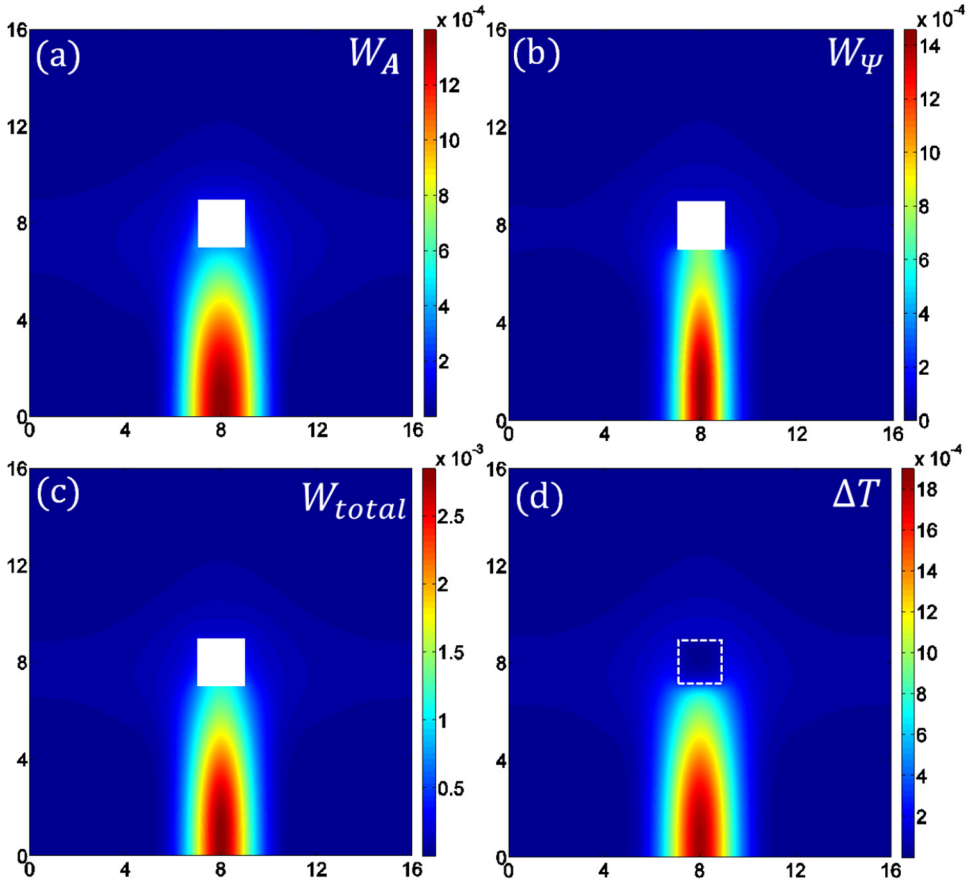

Figure 9. Intensity of the different contributions of dissipated power energy, (a) $W_{\mathbf{A}}$, (b) W_ψ and (c) W_{total}, taken immediately before the annihilation at $T = 0.8T_c$; panel (d) shows the variation of the temperature, ΔT, around the annihilation region. The dissipation and the heat diffusion are concentrated at the regions where the annihilation occurs and is narrower for W_ψ since it originates from the relaxation of ψ.

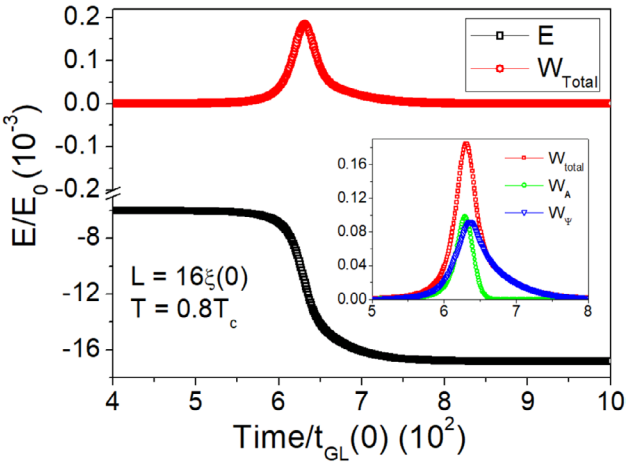

Figure 10. Superconducting (E) and dissipated energy (W_{total}) densities as a function of time in the vicinity of the annihilation for the $L = 16\xi(0)$ sample at $T = 0.8T_c$. The inset shows that the tail of W_{total} is related to the relaxation of ψ after the annihilation, as evidenced by the curves of $W_{\mathbf{A}}$ and W_ψ.

as shown in the lower inset of figure 7. Further ahead this result will be discussed in more detail.

Both the V and the AV acquire a high velocity immediately before the annihilation, and after the collision the energy of the system is reduced. The upper inset of figure 7 shows the variation of the superconducting energy, ΔE, as a function of H/H_{c2} at $T = 0.48T_c$ (dashed line of figure 3). ΔE was evaluated as the difference between the energy immediately before and just after the annihilation. The dips in the range (i) $0.15 < H/H_{c2} < 0.4$ are due to the trapping of a vortex (or two vortices for $L \geqslant 10\xi(0)$) in the hole; (ii) for $0 < H/H_{c2} < 0.14$ in systems with two penetrated vortices, one vortex leaves the sample and a spike is detected; and (iii) the dips around $H = -0.1H_{c2}$ are related to the annihilation of the V–AV pair. The main curve of figure 7 shows the values of the energy dips multiplied by the superconducting area, A_{SC}, as a function of $L/\xi(0)$. Here, $A_{\text{SC}} = L^2 - 2^2$, where 2^2 is the area of the hole in reduced units and $E_0 = \Phi_0^2/32\pi^3\xi(0)\kappa^2$. As we can see, the energy decreases monotonically with $L/\xi(0)$, since the average velocity, v_{avg}, for smaller systems is larger (see lower inset of the same figure).

Another signature of the size effect is the decreasing of v_{avg} as $L/\xi(0)$ is increased (see the lower inset of figure 7). In small samples, the hole is closer to the edge. In this case, the elongation of the vortex and the antivortex cores takes all the region where they are moving and in such degraded region, the pair moves faster. Panels (a) and (b) of figure 8 show the intensity of $|\psi|$ and $\log|\psi|$ with $L = 9\xi(0)$ where one can see that the superconducting state is degraded to some degree all around the sample. On the other hand, the degraded region for larger systems does not take all the extension between the border and the hole. Then, the motion of the V–AV pair

is influenced by the intact superconducting region and v_{avg} decreases as $L/\xi(0)$ increases. For $L \geqslant 11\xi(0)$, v_{avg} becomes nearly independent of the size of the system. In panels 8(c) and (d), the intensity of $|\psi|$ and $\log|\psi|$ for $L = 14\xi(0)$ system present a less degraded region which is responsible for lower v_{avg}. In real units, for the Pb–In compound, v_{avg} is of the order of 10^6 m s^{-1} and such a high velocity is due to the attraction between the V and the AV.

In the next section, we will analyze the kinematic aspects of the annihilation of an Abrikosov's V–AV pair.

3.2. Heat diffusion

The data discussed so far were obtained without taking into account dissipation and heat diffusion processes. When, however, heat transfer is considered, the values of the energy of figure 7 are still valid. In this part of the present study, we simulated similar systems as those ones described previously. We used equations (4) and (5) to estimate the dissipated energy, W_{total}, and the variation of the temperature, $\Delta T/T_c$, during the motion and the annihilation of a V–AV pair. The analysis was carried out for the $L = 16\xi(0)$ sample at $T = 0.8T_c$, $\gamma = 10$ and $u = 5.79$. In figure 9 the intensities of $W_{\mathbf{A}}$, W_ψ, W_{total} and $\Delta T/T_c$ are shown in panels (a)–(d), respectively. The snapshots were taken immediately before the annihilation. As $W_{\mathbf{A}}$ is related to dissipation of normal currents, it takes a wider region in the sample than W_ψ. On the other hand, since W_ψ is due to the relaxation of ψ, a narrower region is dominated by this dissipation mechanism. Recently, Halbertal and coworkers have shown to be possible imaging thermal dissipation in nanoscopic systems by using nanoSQUIDs [57]. Then, our theoretical approach should be experimentally confirmed since ΔT is of the order of $10^{-3}T_c$ (see panel (d)), which is in the sensitivity range of such devices.

It is worth noting in figure 9 that the dissipation and the increase of the temperature are concentrated in the annihilation's region. Additionally, during the annihilation process, there is no subsequent penetration of V–AV pairs.

Figure 10 presents W_{total} and the superconducting energy, E, as a function of time during the annihilation; $W_{total}(t)$ has a tail which is due to the different time scale of $W_{\mathbf{A}}$ and W_ψ and is associated to the relaxation of ψ, as evidenced in the inset of this figure. One can also note that both dissipation mechanisms $W_{\mathbf{A}}$ and W_ψ have the same intensity. As a consequence, both contributions must be taken into account for a better description of the dissipative processes.

Since the magnetization is a measurable quantity, in figure 11, the $M(t)$ curve is shown for the $L = 16\xi(0)$ system and $T = 0.8T_c$. The positive signal of M is due to both the negative applied magnetic field and the vortex trapped in the hole. The insets show the snapshots of $\log|\psi|$ focusing in the region where the V–AV pair is formed. In panel (a) ($t = 5t_{GL}(0)$), it is shown the state where the V is still trapped in the hole; panel (b) ($t = 6.06t_{GL}(0)$) corresponds to the instant when the V leaves the hole; and in panel (c) ($t = 6.21t_{GL}(0)$), the AV penetrates the sample. At $t = 6.23t_{GL}(0)$ (panel (d)) corresponds to the instant of the V–AV collision, i.e. the very moment when the cores of V and AV are superimposed. Just after the annihilation,

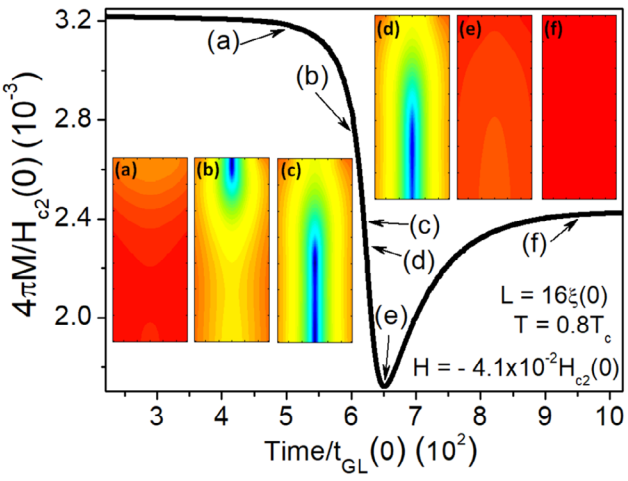

Figure 11. Magnetization as a function of time during the V–AV annihilation process. The snapshots of $\log|\psi|$ show the dynamics of the V–AV pair motion before and after the collision. (a) ($t = 5t_{GL}(0)$) the vortex is trapped in the hole; (b) ($t = 6.06t_{GL}(0)$) the vortex leaves the hole; (c) ($t = 6.2t_{GL}(0)$) the antivortex penetrates the sample; (d) ($t = 6.23t_{GL}(0)$) the V–AV collision; (e) ($t = 6.51t_{GL}(0)$) degradation due to the local heating and (f) ($t = 9.5t_{GL}(0)$) the near recovered superconducting region.

the temperature reaches its maximum value (as shown in figure 9(d)). The local increasing of the temperature generates further degradation of the superconducting state of the surroundings (see the peak of W_{total} in figure 10), as can be seen in panel figure 11(e) at the instant $t = 6.51t_{GL}(0)$. After the annihilation, the system begins to recover the local superconducting state at $t = 9.5t_{GL}(0)$ (see panel (f)). Since M is a response function, its characteristic time is different from that one of the W_{total} and the inflexion of the first one (where the annihilation occurs) does not match with the peak of the last one. After the annihilation, the remained response is due to the surface of the sample. The time during which $M(t)$ changes appreciably is $\delta t \approx 800t_{GL}(0)$, which is of the order of nanoseconds, since $t_{GL} \approx 10^{-13}$ seconds for the Pb–In alloy [56]. Thus, to detect the annihilation of an Abrikosov's V–AV pair using magnetometry would require a device with resolution in the timescale of nanoseconds.

4. Conclusions

In this work we studied the annihilation dynamics of Abrikosov's V–AV pairs in a mesoscopic superconductor with a central hole. In the collision process, the cores of the V and the AV elongates and a phase slip-like (PSlike) appears. In very small samples, $L < 10\xi(0)$, the PSlike degrades superconductivity on the entire region where the pair is moving increasing their average velocity. For systems with $L > 10\xi(0)$, non degraded superconducting regions remain in the moving area implying a lower average velocity. The formation of a V–AV pair and its consequent annihilation in the superconducting region depends on both the size of the system and the temperature. Then, we built an $L(T)$ diagram which can be used as a guide for the predicted occurrence of the annihilation process. The variation of the superconducting energy just before and immediately after the annihilation, multiplied by the superconducting area, increases as the size of the

samples decrease, in accordance with the average velocity of the antivortex, which is lower for larger samples. We coupled the thermal diffusion and the dissipated energies equations to the GTDGL ones. Although, the dissipative term related to the relaxation of the order parameter has been neglected in many works, here we have evidenced that it is a significant contribution to the dissipative processes. We also verified that the time of the V–AV collision is of the order of nanoseconds. Thus, conceivably, the annihilation of Abrikosov's V–AV pairs can be detected by measuring the magnetization response of the sample as a function of time, which would require fast and sensitive detection scheme. Another interesting aspect is that the local increase of the temperature in the annihilation is of the order of $10^{-3}T_c$, which can be measured by a SQUID thermal sensor as described by Halbertal *et al* [57].

Acknowledgments

We thank the Brazilian Agencies CNPq and the São Paulo Research Foundation (FAPESP), grants 2007/08072-0, 2012/04388-0 and 2016/12390-6, for financial support.

References

[1] Berciu M, Rappoport T G and Jankó B 2005 *Nature* **435** 71
[2] Brisbois J *et al* 2016 *Sci. Rep.* **6** 27159
[3] Lopes R F, Carmo D, Colauto F, Ortiz W A, Andrade A M H, Johansen T H, Baggio-Saitovitch E and Pureur P 2017 *J. Appl. Phys.* **121** 013905
[4] Buzdin A I and Brison J P 1994 *Phys. Lett.* A **196** 267
[5] Milošević M V, Kanda A, Hatsumi S, Peeters F M and Ootuka Y 2009 *Phys. Rev. Lett.* **103** 217003
[6] Sardella E and Brandt E H 2010 *Supercond. Sci. Technol.* **23** 025015
[7] Schweigert V A, Peeters F M and Singha Deo P 1998 *Phys. Rev. Lett.* **81** 2783
[8] Melnikov A S, Nefedov I M, Ryzhov D A, Shereshevskii I A, Vinokur V M and Vysheslavtsev P P 2002 *Phys. Rev.* B **65** 140503
[9] Geim A K, Grigorieva I V, Dubonos S V, Lok J G S, Maan J C, Filippov A E and Peeters F M 1997 *Nature* **390** 259
[10] Palacios J J 2000 *Phys. Rev. Lett.* **84** 1796
[11] Misko V R, Xu B and Peeters F M 2007 *Phys. Rev. B.* **76** 024516
[12] Zhao H J, Misko V R, Peeters F M, Oboznov V, Dubonos S V and Grigorieva I V 2008 *Phys. Rev.* B **78** 104517
[13] Golubovic D S, Milošević M V, Peeters F M and Moshchalkov V V 2005 *Phys. Rev.* B **71** 180502
[14] Baelus B J, Peeters F M and Schweigert V A 2001 *Phys. Rev.* B **63** 144517
[15] Sardella E, Lisboa-Filho P N and Malvezzi A L 2008 *Phys. Rev.* B **77** 104508
[16] Kanda A, Baelus B J, Peeters F M, Kadowaki K and Ootuka Y 2004 *Phys. Rev. Lett.* **93** 257002
[17] Mertelj T and Kabanov V V 2003 *Phys. Rev.* B **67** 134527
[18] Chibotaru L F, Ceulemans A, Bruyndoncx V and Moshchalkov V V 2000 *Nature* **408** 833
[19] Geurts R, Milošević M V and Peeters F M 2009 *Phys. Rev.* B **79** 174508
[20] Sardella E, Lisboa-Filho P N, Silva C C S, Cabral L R E and Ortiz W A 2009 *Phys. Rev.* B **80** 012506
[21] Zadorosny R, Duarte E C S, Sardella E and Ortiz W A 2014 *Physica* C **503** 94
[22] Milošević M V, Peeters F M and Jankó B 2011 *Supercond. Sci. Technol.* **24** 024001
[23] Gomes A, Gonzalez E M, Gilbert D A, Milošević M V, Kai Liu and Vicent J L 2013 *Supercond. Sci. Technol.* **26** 085018
[24] Kramer R B G, Silhanek A V, Gillijns W and Mochshalkov V V 2011 *Phys. Rev.* X **1** 021004
[25] Kapra A V, Misko V R, Vodolazov D Y and Peeters F M 2011 *Supercond. Sci. Technol.* **24** 024014
[26] Gladilin V N, Tempere J, Devreese J T and Moshchalkov V V 2012 *New J. Phys.* **14** 103021
[27] Shapiro I, Pechenik E and Shapiro B Ya 2001 *Phys. Rev.* B **63** 184520
[28] Ghinovker M, Shapiro B Ya and Shapiro I 2001 *Europhys. Lett.* **53** 240
[29] Aranson I, Gitterman M and Shapiro B Ya 1995 *Phys. Rev.* B **51** 3092
[30] Aranson I, Shapiro B Ya and Vinokur V 1996 *Phys. Rev. Lett.* **76** 142
[31] Berdiyorov G R, Milošević M V and Peeters F M 2009 *Phys. Rev.* B **79** 184506
[32] Gulevich D R and Kusmartsev F V 2007 *New J. Phys.* **9** 59
[33] Eom B H, Day P K, LeDuc H G and Zmuidzinas J 2012 *Nat. Phys.* **8** 623
[34] Vasyukov D *et al* 2013 *Nat. Nanotechnol.* **8** 639
[35] Rosticher M, Maneval F R, Dorenbos S N, Zijlstra T, Klapwijk T M, Zwiller V, Lupascu A and Nogues G 2010 *Appl. Phys. Lett.* **97** 183106
[36] Gol'tsman G N, Okunev O, Chulkova G, Lipatov A, Semenov A, Smirnov K, Voronov B, Dzardanov A, Williams C and Sobolewski R 2001 *Appl. Phys. Lett.* **79** 705
[37] Kerman A J, Dauler E A, Yang J K W, Rosfjord K M, Anant V, Berggren K K, Gol'tsman G N and Boronov B M 2007 *Appl. Phys. Lett.* **90** 101110
[38] Salim A J, Eftekharian A and Majedi A H 2014 *J. Appl. Phys.* **115** 054514
[39] Berdiyorov G R, Milošević M V and Peeters F M 2012 *Appl. Phys. Lett.* **100** 262603
[40] Schmid A 1966 *Phys. Kondens. Mater.* **5** 302
[41] Petković I, Lollo A, Glazman L I and Harris J G E 2016 *Nat. Commun.* **7** 13551
[42] Vodolazov D Y, Peeters F M, Morelle M and Moshchalkov V V 2005 *Phys. Rev.* B **71** 184502
[43] Berdiyorov G R, Chao X C, Peeters F M, Wang H B, Moshchalkov V V and Zhu B Y 2012 *Phys. Rev.* B **86** 224504
[44] Berdiyorov G R, Milošević M V, Latimer M L, Xiao Z L, Kwok W K and Peeters F M 2012 *Phys. Rev. Lett.* **109** 057004
[45] Hernandez A D and Dominguez D 2008 *Phys. Rev.* B **77** 224505
[46] Kramer L and Watts-Tobin R J 1978 *Phys. Rev. Lett.* **40** 1041
[47] Kramer L and Baratoff A 1977 *Phys. Rev. Lett.* **38** 518
[48] Gor'kov L P and Èliasberg G M 1968 *Sov. Phys.—JETP* **27** 328
[49] Gor'kov L P and Kopnin N B 1975 *Sov. Phys.—Usp.* **18** 496
[50] Gropp W D, Kaper H G, Leaf G K, Levine D M, Palumbo M and Vinokur V M 1996 *J. Comput. Phys.* **123** 254
[51] Milošević M V and Geurts E 2010 *Physica* C **470** 791
[52] Kogut J 1979 *Rev. Mod. Phys.* **51** 659
[53] Baranov V V, Balanov A G and Kabanov V V 2011 *Phys. Rev.* B **84** 094527
[54] Ivlev B I, Kopnin N B and Maslova L A 1980 *Sov. Phys. JETP* **51** 986 (http://www.jetp.ac.ru/cgi-bin/dn/e_051_05_0986.pdf)
[55] Ivlev B I, Kopnin N B and Larkin L A 1985 *Sov. Phys. JETP* **61** 337 (http://www.jetp.ac.ru/cgi-bin/dn/e_061_02_0337.pdf)
[56] Poole C P Jr, Farach H A, Creswick R J and Prozorov R 2007 *Superconductivity* 2nd edn (Amsterdam: Elsevier)
[57] Halbertal D *et al* 2016 *Nature* **539** 470